

Investigation of the Spectroscopic, Electrochemical, and Spectroelectrochemical Properties of Osmium(II) Complexes Incorporating Polyazine Bridging Ligands: Formation of the Os/Os and Os/Ru Mixed-Valence Complexes

Mark M. Richter[†] and Karen J. Brewer^{*}

Department of Chemistry, Virginia Polytechnic Institute and State University,
Blacksburg, Virginia 24061-0212

Received November 25, 1992

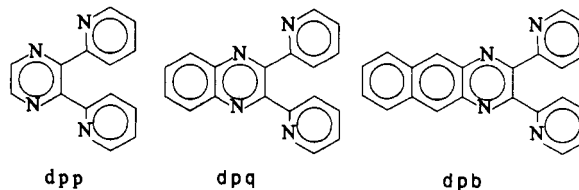
A series of homobimetallic Os(II) complexes have been prepared of general formula $[(\text{bpy})_2\text{Os}]_2(\text{BL})^{4+}$ (where BL = bridging ligand and bpy = 2,2'-bipyridine). The bridging ligands used were 2,3-bis(2-pyridyl)pyrazine (dpp), 2,3-bis(2-pyridyl)quinoxaline (dpq), and 2,3-bis(2-pyridyl)benzoquinoxaline (dpb). The compounds' electrochemical, spectroscopic, and spectroelectrochemical properties have been studied and comparisons have been made with previously prepared Os/Ru heterobimetallic and Ru/Ru homobimetallic complexes incorporating the same bridging ligands. The lowest energy electronic transitions in these homometallic systems have been assigned as $\text{Os}(\text{d}\pi) \rightarrow \text{BL}(\pi^*)^1\text{MLCT}$ transitions. On the basis of spectroelectrochemical experiments, assignments for the electronic absorption spectra have been made. The Os(II)/Os(III) and Os(III)/Ru(II) mixed-valence complexes of this series of ligands have been prepared. These mixed-valence systems display rich near-infrared spectra. Values for the extent of electron delocalization between the metal centers, α^2 , range from 2.7×10^{-3} to 1.0×10^{-2} , which indicates that these systems are much more weakly coupled Robin and Day class II systems than has been previously implied through electrochemical analysis.

Introduction

Monometallic ruthenium(II) and osmium(II) polypyridine complexes have been shown to display intense metal-to-ligand charge-transfer (MLCT) transitions well into the visible region of the spectrum.¹ Substitution of polyazine bridging ligands such as dpp, dpq, and dpb for bipyridine in these systems tends to significantly red-shift the MLCT transitions as a result of a lowering of the π^* -acceptor orbital of the ligand.^{1a,b,2-15} These monometallic bridging-ligand complexes have been used to prepare a number of homometallic ruthenium(II) polypyridyl-bridged complexes^{1a,b,2,5,8,16-19} as well as a few osmium(II) bimetallic systems,^{3,4,20,21} including $[(\text{bpy})_2\text{Os}]_2(\text{dpp})^{4+}$ (bpy = 2,2'-bipyridine), which has previously been prepared by

Campagna and co-workers.²¹ Several studies have been done comparing the electrochemical and spectral properties of the monometallic $[(\text{bpy})_2\text{Ru}(\text{BL})]^{2+}$ systems with the bimetallic $[(\text{bpy})_2\text{Ru}]_2(\text{BL})^{4+}$ complexes where BL can be one of several polypyridyl ligands. These studies have shown that the metal complexes of interest are strongly affected by the identity of the bridging ligand and the number of metals involved in the system. Electrochemical studies of homometallic systems have yielded large values of K_{com} .^{1a,b,4,8}

Within this framework, we have synthesized complexes of the type $[(\text{bpy})_2\text{Os}]_2(\text{BL})^{4+}$, where BL = bridging ligand (dpp, dpq, or dpb). These three ligands differ from each other only by



the addition of electron-withdrawing benzene groups fused to the side of the pyrazine ring. This results in a net stabilization of the lowest-unoccupied π^* orbital and makes possible the development of a series of compounds in which properties that are not directly related to the BL-based orbital energies are not significantly altered by bridging-ligand substitution.

Experimental Section²²

Materials. The materials were of reagent grade and were used without further purification. The ligand 2,3-bis(2-pyridyl)pyrazine (dpp) was

* Author to whom correspondence should be addressed.
[†] Department of Chemistry, Washington State University, Pullman, WA 99164-4630.

- (a) Braunstein, C. H.; Baker, A. P.; Streckas, T. C.; Gafney, H. D. *Inorg. Chem.* **1984**, *23*, 857. (b) Rillema, D. P.; Mack, K. B. *Inorg. Chem.* **1982**, *21*, 3849. (c) Kober, E. M.; Caspar, J. P.; Sullivan, B. P.; Meyer, T. J. *Inorg. Chem.* **1988**, *27*, 4587 and references therein. (d) Lumpkin, R. S.; Kober, E. M.; Worl, L. A.; Murtaza, Z.; Meyer, T. J. *J. Phys. Chem.* **1990**, *94*, 239. (e) Kober, E. M.; Marshall, J. L.; Dressick, W. J.; Sullivan, B. P.; Caspar, J. V.; Meyer, T. J. *Inorg. Chem.* **1985**, *24*, 2755 and references therein. (f) Pinnick, D.; Durham, B. *Inorg. Chem.* **1984**, *23*, 1440.
- Cooper, J. B.; MacQueen, D. B.; Petersen, J. D.; Wertz, D. W. *Inorg. Chem.* **1990**, *29*, 3701.
- Kalyanasundaram, K.; Nazeeruddin, Md. K. *Chem. Phys. Lett.* **1989**, *158*, 45.
- (a) Richter, M. M.; Brewer, K. J. *Inorg. Chem.* **1992**, *31*, 1594. (b) Richter, M. M.; Brewer, K. J. *Inorg. Chim. Acta* **1991**, *180*, 125.
- Dose, E. V.; Wilson, L. J. *Inorg. Chem.* **1978**, *17*, 2660.
- Huziker, B.; Ludi, A. *J. Am. Chem. Soc.* **1977**, *99*, 7370.
- Ruminski, R. R.; Petersen, J. D. *Inorg. Chem.* **1982**, *21*, 3706.
- Petersen, J. D. In *Supramolecular Photochemistry*; Balzani, V., Ed.; Reidel: Norwell, MA, 1987; p 135.
- Kaim, W.; Ernst, S. *J. Am. Chem. Soc.* **1986**, *108*, 3578.
- Kaim, W.; Kohlman, S. *Inorg. Chem.* **1987**, *26*, 68.
- DeCola, L.; Barigelletti, F. *Gazz. Chim. Ital.* **1988**, *118*, 417.
- Campagna, S.; Denti, G.; De Rosa, G.; Sabatino, L.; Ciano, M.; Balzani, V. *Inorg. Chem.* **1989**, *28*, 2565.
- Sahai, R.; Morgan, L.; Rillema, P. *Inorg. Chem.* **1988**, *27*, 3495.
- Fuchs, Y.; Lofters, S.; Dieter, T.; Shi, W.; Morgan, R.; Streckas, T.; Gafney, H.; Baker, D. *J. Am. Chem. Soc.* **1987**, *109*, 2691.
- Hosok, W.; Tysoe, S.; Gafney, H.; Baker, D.; Streckas, T. *Inorg. Chem.* **1989**, *28*, 1228.

- Brewer, K. J.; Murphy, W. R.; Spurlin, S. R.; Petersen, J. D. *Inorg. Chem.* **1986**, *25*, 882.
- Rillema, D. P.; Callahan, R. W.; Mack, K. B. *Inorg. Chem.* **1982**, *21*, 2589.
- Petersen, J. D.; Murphy, W. R.; Brewer, K. J.; Ruminski, R. R. *Coord. Chem. Rev.* **1985**, *64*, 261 and references therein.
- Murphy, W. R.; Brewer, K. J.; Gettcliffe, G.; Petersen, J. D. *Inorg. Chem.* **1989**, *28*, 81.
- (a) Schanze, K. S.; Neyhart, G. A.; Meyer, T. J. *J. Phys. Chem.* **1986**, *90*, 2182. (b) Goldsby, K. A.; Meyer, T. J. *Inorg. Chem.* **1984**, *23*, 3002.
- Denti, G.; Serroni, S.; Sabatino, L.; Ciano, M.; Recevuto, V.; Campagna, S. *Gazz. Chim. Ital.* **1991**, *121*, 37.

purchased from Aldrich Chemical Co. The ligands 2,3-bis(2-pyridyl)-quinoxaline (dpq) and 2,3-bis(2-pyridyl)benzoquinoxaline were synthesized according to literature procedures.^{23,24} The acetonitrile used in the electrochemical measurements was of Spectroquality grade (Burdick and Jackson), and the supporting electrolyte used, tetrabutylammonium hexafluorophosphate (Bu_4NPF_6), was prepared from tetrabutylammonium bromide and HPF_6 (Aldrich), recrystallized several times from ethanol, and stored in a vacuum desiccator prior to use. All other chemicals were from Fisher Scientific.

Syntheses. $[\text{Os}(\text{bpy})_2(\text{BL})](\text{PF}_6)_2$,^{4b} $[\text{Os}(\text{bpy})_2\text{Cl}_2]$,²⁵ and $[[(\text{bpy})_2\text{Ru}]_2(\text{BL})](\text{PF}_6)_4$ (BL = dpp, dpq, dpb) were prepared as described previously.^{1a,b,26}

$[[(\text{bpy})_2\text{Os}]_2(\text{dpp})](\text{PF}_6)_4 \cdot 2\text{H}_2\text{O}$ was prepared by a modification of the synthesis of Campagna et al.²¹ by reacting approximately 2.5 equiv of $\text{Os}(\text{bpy})_2\text{Cl}_2$ (0.600 mmol, 0.344 g) with 1 equiv of the ligand dpp (0.240 mmol, 0.056 g) in 30 mL of ethylene glycol for approximately 45 min. The flask was then removed from the heat, and a saturated solution of aqueous KPF_6 (75 mL) was added with stirring to induce precipitation. The precipitate was collected by vacuum filtration. The product was purified by column chromatography on neutral alumina using a 2:1 (v/v) toluene/acetonitrile eluent to load the product onto the column. The purple product band was the third to elute. The first two bands were eluted using the 2:1 (v/v) toluene/acetonitrile mixture mentioned above whereas it was necessary to use a 1:2 (v/v) toluene/acetonitrile mixture to elute the product band. The product was collected, concentrated by rotary evaporation, and precipitated by addition to a stirred solution of diethyl ether (200 mL). The precipitate was then collected by vacuum filtration, washed with diethyl ether, and dried under vacuum. The chromatographic procedure was repeated twice to ensure product purity. Typical yield: 56%. Anal. Calcd: C, 34.95; H, 2.50; N, 9.06. Found: C, 35.05; H, 2.58; N, 9.00.

$[[(\text{bpy})_2\text{Os}]_2(\text{dpq})](\text{PF}_6)_4 \cdot 2\text{H}_2\text{O}$ was prepared as above with dpq (0.240 mmol, 0.0682 g) substituted for dpp. The reddish/purple product band was the third to elute. The first two bands were eluted using the 2:1 (v/v) toluene/acetonitrile mixture mentioned above whereas a 1:3 (v/v) toluene/acetonitrile mixture was used to elute the product band. It was necessary to repeat the chromatographic procedure four times to ensure product purity. Typical yield: 58%. Anal. Calcd: C, 36.55; H, 2.54; N, 8.82. Found: C, 36.61; H, 2.65; N, 8.98.

$[[(\text{bpy})_2\text{Os}]_2(\text{dpb})](\text{PF}_6)_4 \cdot 3\text{H}_2\text{O}$ was prepared as above with the ligand dpb (0.240 mmol, 0.081 g) substituted for dpq. The green product band was the fourth to elute. The first two bands were eluted using the 2:1 (v/v) toluene/acetonitrile mixture mentioned above and the third band was eluted using a 1:1 (v/v) toluene/acetonitrile mixture whereas a 1:4 (v/v) toluene/acetonitrile solvent mixture was used to elute the product band. It was necessary to repeat the chromatographic procedure four times to ensure product purity. Typical yield: 43%. Anal. Calcd: C, 37.56; H, 2.67; N, 8.48. Found: C, 37.60; H, 2.56; N, 8.32.

Physical Measurements. The configuration of the experiments for the cyclic and Osteryoung square-wave voltammograms,⁴ UV/vis absorption spectroscopy,⁴ and spectroelectrochemistry²⁷ have been described in detail elsewhere. All measurements were made on acetonitrile or dimethylformamide (DMF) solutions at room temperature.

Results and Discussion

Electrochemistry. Cyclic voltammograms of the monometallic Os(II) and Ru(II) complexes, $[\text{M}(\text{bpy})_2(\text{BL})]^{2+}$ (BL = dpp, dpq, dpb), in acetonitrile, are consistent with three ligand-based reductions and one metal-based oxidation.^{1a,b,2-15} The first reduction in each case corresponds to reduction of the bridging ligand and shifts to more positive potential on going from dpp to dpq to dpb. The second and third reductions correspond to subsequent reductions of the two bipyridine ligands.⁴

Cyclic voltammograms of the bimetallic Os(II)/Ru(II) mixed-metal complexes, $[[(\text{bpy})_2\text{Os}(\text{BL})\text{Ru}(\text{bpy})_2]^{4+}$ (BL = dpp, dpq, dpb), are consistent with two reversible metal-based oxidations

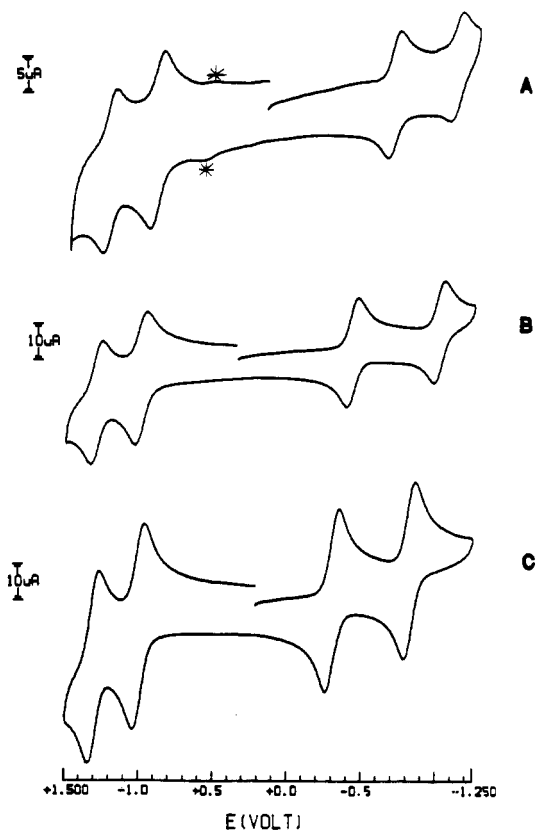


Figure 1. Cyclic voltammograms (CH_3CN containing 0.1 M Bu_4NPF_6): (A) $[[(\text{bpy})_2\text{Os}]_2(\text{dpp})](\text{PF}_6)_4$; (B) $[[(\text{bpy})_2\text{Os}]_2(\text{dpq})](\text{PF}_6)_4$; (C) $[[(\text{bpy})_2\text{Os}]_2(\text{dpb})](\text{PF}_6)_4$. The starred peaks in part A are noticeably absent when the scan is reversed after only one reduction is allowed to occur. The appearance of the peaks after two-electron reduction is indicative of decomposition products.

and six reversible ligand-based reductions. In all of the bimetallic complexes, the first and second reductions have been shown to be BL based.^{3,4a} The oxidative processes involve oxidation of Os(II) to Os(III) and Ru(II) to Ru(III) with the Ru(II)/Ru(III) oxidation occurring approximately 500 mV more anodic than the corresponding Os(II)/Os(III) oxidation.^{3,4a,38}

The Ru(II) bimetallic complexes, $[[(\text{bpy})_2\text{Ru}]_2(\text{BL})]^{4+}$ (BL = dpp, dpq, dpb), each display two reversible oxidations and six reversible reductions in the potential window from +1.90 to -2.00 V.^{1a,b,26} In each of the complexes, the first reduction is BL based. Recently, Berger has shown via spectroelectrochemical experiments on $[\text{Ru}(\text{bpy})_2(\text{dpp})]^{2+}$ and $[[(\text{bpy})_2\text{Ru}]_2(\text{dpp})]^{4+}$ that the second reduction in the bimetallic complex corresponds to reduction of the dpp ligand by a second electron.²⁸ The subsequent four reductions have been assigned to sequential reductions of the four bipyridine ligands by one electron each.^{2,28} The oxidative processes correspond to sequential oxidations of the two ruthenium centers by one electron each.

The cyclic voltammograms of the three homometallic Os(II) complexes, $[[(\text{bpy})_2\text{Os}]_2(\text{BL})]^{4+}$, are shown in Figure 1 and the electrochemical data given in Table I. In acetonitrile, the dpp, dpq, and dpb bimetallic complexes each display two reversible oxidations and two reversible reductions in the potential region from +1.50 to -1.20 V vs Ag/AgCl. The subsequent reductions, corresponding to reduction of the four bipyridine ligands, are not well-behaved probably due to the adsorption of the quadruply reduced species onto the surface of the electrode. Adsorption and desorption spikes persist at scan rates as high as 8 V/s. In DMF, the adsorption and desorption spikes disappear and the bimetallic complexes display six reversible reductions in the potential window from 0.0 to -2.0 V vs Ag/AgCl. It was not possible to observe the oxidative waves in DMF due to oxidation

- (22) Experimental work performed at Washington State University.
 (23) Goodwin, H. A.; Lions, F. *J. Am. Chem. Soc.* **1959**, *81*, 6415.
 (24) Bairo, A. J.; Carlson, D. L.; Wolosh, G. M.; DeJesus, D. E.; Knowles, C. F.; Szabo, E. G.; Murphy, W. R. *Inorg. Chem.* **1990**, *29*, 2327.
 (25) Buckingham, D. A.; Dwyer, F. P.; Goodwin, H. A.; Sargeson, A. M. *Aust. J. Chem.* **1964**, *17*, 325.
 (26) Carlson, D. C.; Murphy, W. R. *Inorg. Chim. Acta*, in press.
 (27) Brewer, K. J.; Lumpkin, R. S.; Otvos, J. W.; Spreer, L. O.; Calvin, M. *Inorg. Chem.* **1989**, *28*, 4446.

- (28) Berger, R. M. *Inorg. Chem.* **1990**, *29*, 1920.

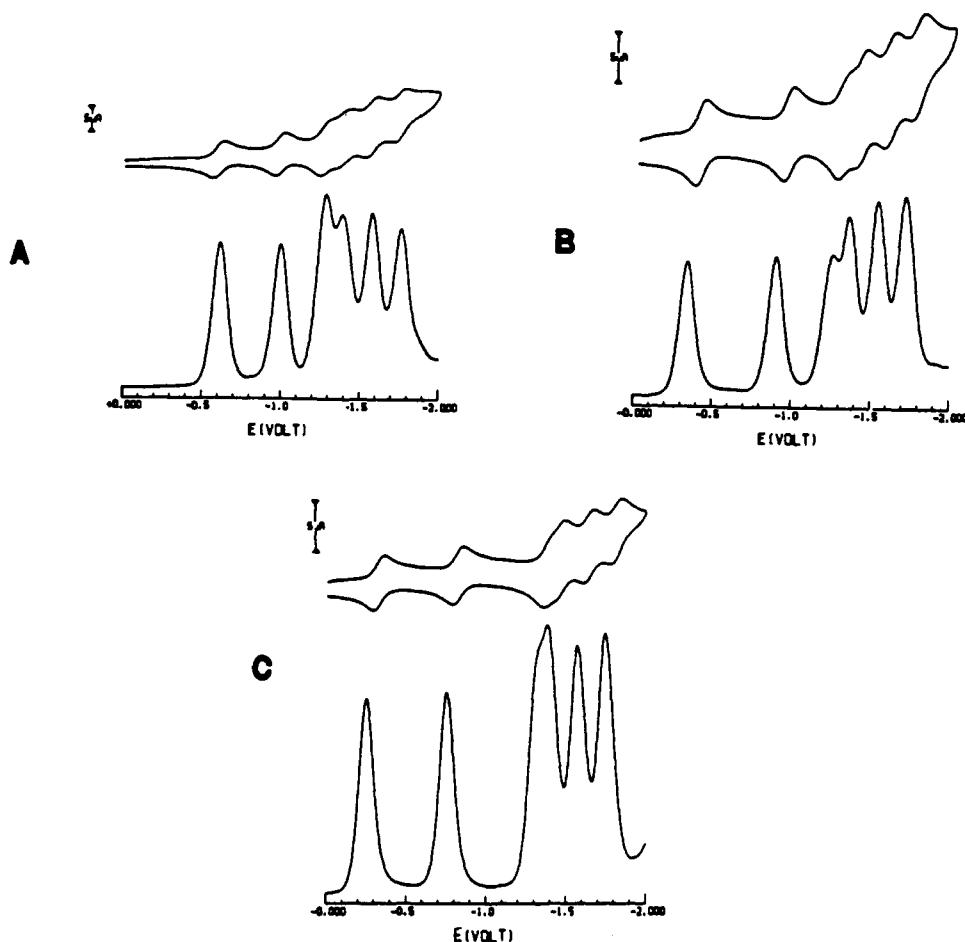


Figure 2. Cyclic and Osteryoung square-wave voltammograms (DMF containing 0.1 M Bu_4NPF_6): (A) $[[(\text{bpy})_2\text{Os}]_2(\text{dpp})](\text{PF}_6)_4$; (B) $[[(\text{bpy})_2\text{Os}]_2(\text{dpq})](\text{PF}_6)_4$; (C) $[[(\text{bpy})_2\text{Os}]_2(\text{dpb})](\text{PF}_6)_4$.

of the solvent. The electrochemical data for the complexes in DMF are given in Table I, and the cyclic and Osteryoung square-wave voltammograms are shown in Figure 2. The proposed electrochemical reactions are given in Scheme I.

Addition of the second $\text{Os}(\text{bpy})_2^{2+}$ fragment through the remote nitrogens on the bridging ligands results in anodic shifts of the first BL reduction of 340, 320, and 280 mV for $[[(\text{bpy})_2\text{Os}]_2(\text{dpp})]^{4+}$, $[[(\text{bpy})_2\text{Os}]_2(\text{dpq})]^{4+}$, and $[[(\text{bpy})_2\text{Os}]_2(\text{dpb})]^{4+}$, respectively, as compared with the osmium monometallic precursor complexes in acetonitrile. These shifts reflect a net stabilization of the π^* orbitals of the bridging ligands in the bimetallic complexes relative to the π^* orbitals of the BL in the monometallic complexes. The second reduction in these complexes is assigned as the second reduction of the bridging ligand by comparison with the previously prepared Os/Ru heterobimetallic complexes and Ru/Ru homobimetallic complexes. After reduction of the BL by two electrons, we expected to observe reduction of the bipyridine ligands. The four equivalent bpy ligands reduce at different potentials, indicative of a significant degree of electronic coupling. This is somewhat surprising since the first bpy ligands reduced must couple through an Os(BL)Os framework. The ruthenium analogs of these compounds also display four bpy-based reductions at roughly the same potentials as the osmium complexes, giving further support to their assignment as being bipyridine based.^{1a,b,2,26,28}

The oxidative processes involve sequential oxidations of the Os(II) centers to Os(III) with the second oxidation occurring approximately 300 mV more positive than the first. These assignments were made by analogy to the monometallic $[\text{Os}(\text{bpy})_2(\text{BL})]^{2+}$ and previously prepared homo- and heterobimetallic systems.^{3,4,20,21} We have recently shown that the change in the ligand field about the metal ion caused by the variation in the bridging ligand produces small changes in the osmium

Table I. Cyclic Voltammetric Data for Osmium Polypyridyl Complexes^a

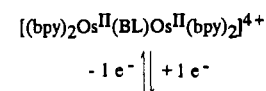
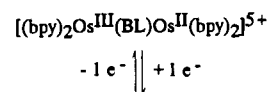
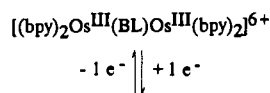
complex	solvent	$E_{1/2}$ (V)	assgnt
$[[(\text{bpy})_2\text{Os}]_2(\text{dpp})]^{4+}$	CH_3CN	+1.22	$\text{Os}^{\text{III}}, \text{Os}^{\text{II}} / \text{Os}^{\text{III}}, \text{Os}^{\text{III}}$
		+0.91	$\text{Os}^{\text{II}}, \text{Os}^{\text{II}} / \text{Os}^{\text{III}}, \text{Os}^{\text{II}}$
		-0.68	dpp/dpp ⁻
		-1.06	dpp ⁻ /dpp ²⁻
		-1.28	bpy/bpy ⁻
	DMF	-0.61	dpp/dpp ⁻
		-1.00	dpp ⁻ /dpp ²⁻
		-1.28	bpy/bpy ⁻
		-1.38	bpy/bpy ⁻
		-1.58	bpy/bpy ⁻
$[[(\text{bpy})_2\text{Os}]_2(\text{dpq})]^{4+}$	CH_3CN	+1.28	$\text{Os}^{\text{III}}, \text{Os}^{\text{II}} / \text{Os}^{\text{III}}, \text{Os}^{\text{III}}$
		+0.98	$\text{Os}^{\text{II}}, \text{Os}^{\text{II}} / \text{Os}^{\text{III}}, \text{Os}^{\text{II}}$
		-0.44	dpq/dpq ⁻
		-1.03	dpq ⁻ /dpq ²⁻
		-1.26	bpy/bpy ⁻
	DMF	-0.34	dpq/dpq ⁻
		-0.90	dpq ⁻ /dpq ²⁻
		-1.26	bpy/bpy ⁻
		-1.36	bpy/bpy ⁻
		-1.54	bpy/bpy ⁻
$[[(\text{bpy})_2\text{Os}]_2(\text{dpb})]^{4+}$	CH_3CN	+1.30	$\text{Os}^{\text{III}}, \text{Os}^{\text{II}} / \text{Os}^{\text{III}}, \text{Os}^{\text{III}}$
		+0.98	$\text{Os}^{\text{II}}, \text{Os}^{\text{II}} / \text{Os}^{\text{III}}, \text{Os}^{\text{II}}$
		-0.33	dpb/dpb ⁻
		-0.85	dpb ⁻ /dpb ²⁻
		-1.26	bpy/bpy ⁻
	DMF	-0.25	dpb/dpb ⁻
		-0.76	dpb ⁻ /dpb ²⁻
		-1.31	bpy/bpy ⁻
		-1.39	bpy/bpy ⁻
		-1.58	bpy/bpy ⁻
-1.74	bpy/bpy ⁻		

^a Potentials were recorded versus a Ag/AgCl reference electrode (0.268 V vs SHE) in 0.1 M Bu_4NPF_6 at a scan rate of 200 mV/s.

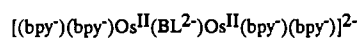
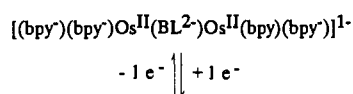
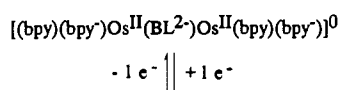
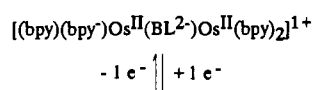
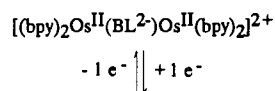
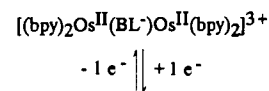
oxidation potentials.⁴ We would therefore expect that significant changes in the metal oxidation potential would be the result of

Scheme I

Oxidative Processes



Reductive Processes



the addition of the second metal center. The presence of two one-electron oxidations, in lieu of one two-electron oxidation, indicates a stabilization of the mixed-valence species. The separation between the two oxidation potentials ($\Delta E_{1/2} = E_{1/2}(\text{M}^{\text{III}}, \text{M}^{\text{III}}/\text{M}^{\text{III}}, \text{M}^{\text{II}}) - E_{1/2}(\text{M}^{\text{III}}, \text{M}^{\text{II}}/\text{M}^{\text{II}}, \text{M}^{\text{II}})$) has been shown to be related to the structural and electronic properties of the BL.^{14,20,29-31} The value of 300 mV found by Campagna et al.²¹ for $[(\text{bpy})_2\text{Os}]_2(\text{dpp})^{4+}$ and by us for the dpq and dpb derivatives indicates a significant degree of stabilization of the mixed-valence species as well as showing that the structural differences between dpp, dpq, and dpb do not appear to significantly influence this stabilization within this series of complexes. Values for the homometallic Ru^{II} complexes range from 180 mV for $[(\text{bpy})_2\text{Ru}]_2(\text{dpp})^{4+}$ and $[(\text{bpy})_2\text{Ru}]_2(\text{dpb})^{4+}$ to 150 mV for $[(\text{bpy})_2\text{Ru}]_2(\text{dpq})^{4+}$, indicating significantly enhanced stabilization in the osmium systems. The separation between the two oxidation potentials, $\Delta E_{1/2}$, also gives a quantitative measure of the energetics for the comproportionation reaction ($K_{\text{com}} = e^{\Delta E_{1/2}(\text{mV})/25.69}$ at T = 298 K).



K_{com} values range from 4 in the uncoupled Robin and Day Class I systems to $>10^{13}$ in strongly coupled Class III systems.^{29,32}

Table II. Electronic Spectral Data for a Series of Bimetallic Os(II) Complexes Containing Polypyridine Bridging Ligands^a

complex	$\lambda_{\text{max}}^{\text{abs}}$ (nm)	$10^{-3}\epsilon$ ($\text{M}^{-1} \text{cm}^{-1}$)	assgnt
$[(\text{bpy})_2\text{Os}]_2(\text{dpp})^{4+}$	286	96.7	$\pi \rightarrow \pi^*(\text{bpy})$
	356 (sh)	26.4	$\pi \rightarrow \pi^*(\text{dpp})$
	432	19.8	¹ MLCT(bpy)
	552	25.2	¹ MLCT(dpp)
$[(\text{bpy})_2\text{Os}]_2(\text{dpq})^{4+}$	286	90.5	$\pi \rightarrow \pi^*(\text{bpy})$
	356 (sh)	21.7	$\pi \rightarrow \pi^*(\text{dpq})$
	398	19.6	¹ MLCT(dpq)
	428	14.3	¹ MLCT(bpy)
$[(\text{bpy})_2\text{Os}]_2(\text{dpb})^{4+}$	630	20.9	¹ MLCT(dpq)
	286	90.7	$\pi \rightarrow \pi^*(\text{bpy})$
	354	35.3	$\pi \rightarrow \pi^*(\text{dpb})$
	422	16.6	¹ MLCT(bpy)
	510	8.16	¹ MLCT(dpq)
	610	12.9	¹ MLCT(dpq)
	670	16.8	¹ MLCT(dpq)

^a Spectra were recorded in CH₃CN at room temperature.

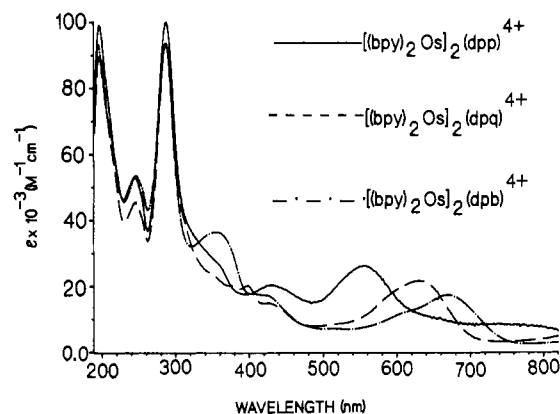


Figure 3. Electronic absorption spectra for a series of Os(II) polypyridyl complexes in CH₃CN.

Values for the bimetallic complexes in question are 1.7×10^5 for $[(\text{bpy})_2\text{Os}]_2(\text{dpp})^{4+}$, 1.2×10^5 for $[(\text{bpy})_2\text{Os}]_2(\text{dpq})^{4+}$, and 2.6×10^5 for $[(\text{bpy})_2\text{Os}]_2(\text{dpb})^{4+}$ as compared with 1.1×10^3 for $[(\text{bpy})_2\text{Ru}]_2(\text{dpp})^{4+}$, 3.4×10^2 for $[(\text{bpy})_2\text{Ru}]_2(\text{dpq})^{4+}$, and 1.1×10^3 for $[(\text{bpy})_2\text{Ru}]_2(\text{dpb})^{4+}$.^{1a,b,26} These results indicate that both the ruthenium and osmium complexes may be classified as Class II systems with the osmium systems being more strongly coupled than the analogous ruthenium systems. This enhanced coupling of the osmium complexes results from the higher energy of the $d\pi$ osmium orbitals. This facilitates mixing with the bridging-ligand-based π^* orbitals, giving rise to a more strongly coupled bimetallic system.

Electronic Absorption Spectroscopy. The electronic spectral data for each of the Os(II) bimetallic complexes are summarized in Table II and shown in Figure 3. The electronic spectrum of $[(\text{bpy})_2\text{Os}]_2(\text{dpp})^{4+}$ has been previously reported by Campagna and co-workers.²¹ The values reported are those obtained by us to make comparisons among the systems more valid.

In general, mixed polypyridyl complexes of Ru(II) and Os(II) exhibit multiple absorptions in the visible region of the spectrum, where the separation between the bands reflects the difference between the π systems of the ligands.^{1a,14} In the monometallic osmium and ruthenium compounds, $[\text{M}(\text{bpy})_2(\text{BL})]^{2+}$ (BL = dpp, dpq, dpb; M = Os, Ru), the UV region of the spectrum exhibits $\pi \rightarrow \pi^*$ transitions which are both bpy and BL based. Each complex has bands at lower energies due to both $n \rightarrow \pi^*$ and metal-to-bpy charge transfers and displays metal-to-bridging ligand charge-transfer bands in the visible region which shift to lower energy upon going from dpp to dpq to dpb, respectively.

The Os(II)/Os(II) complexes display several overlapping bands in both the UV and visible regions. The intense higher energy band at approximately 286 nm for each of the three complexes is assigned as a bpy-centered $\pi \rightarrow \pi^*$ transition by analogy to the free-ligand spectra, which is consistent with this transition

(29) Creutz, C. *Prog. Inorg. Chem.* **1983**, *30*, 1.

(30) DeCola, L.; Ciano, M.; Barigelletti, F.; Garcia, M. P.; Oro, L. A. *Inorg. Chim. Acta* **1990**, *172*, 181.

(31) Barigelletti, F.; Juris, A.; Balzani, V.; Belser, P.; Von Zelewsky, A. J. *Phys. Chem.* **1987**, *91*, 1095.

(32) Robin, M. B.; Day, P. *Adv. Inorg. Radiochem.* **1967**, *10*, 247.

(33) Molnar, S. M.; Jensen, G. E.; Neville, K.; Brewer, K. J. *Inorg. Chim. Acta* **1992**, *206*, 69.

being present regardless of the bridging ligand or metal employed (i.e. dpp, dpq, or dpb and Os or Ru) in both the mono- and bimetallic complexes studied to date.^{2-4,20,24}

Lower in energy than the bpy-centered $\pi \rightarrow \pi^*$ transitions are a series of BL-based $\pi \rightarrow \pi^*$ and $n \rightarrow \pi^*$ absorptions which appear at 356 nm for $[(\text{bpy})_2\text{Os}]_2(\text{dpp})^{4+}$, 378 nm for $[(\text{bpy})_2\text{Os}]_2(\text{dpq})^{4+}$, and 408 nm for $[(\text{bpy})_2\text{Os}]_2(\text{dpb})^{4+}$. These bridging-ligand-centered transitions are slightly red-shifted (as compared with the spectra of the free ligands and monometallic complexes) upon coordination of the second metal fragment.

The bands in the visible region consist of a series of MLCT transitions which are both bpy and BL based. The lowest energy bands (at 552, 630, and 670 nm for the dpp, dpq, and dpb complexes, respectively) consist of $\text{Os}(\text{d}\pi) \rightarrow \text{BL}(\pi^*)$ MLCT transitions which can be assigned by comparison with monometallic and previously prepared multimetallic complexes.^{1d-f,2-4,20,24,34,35} The lowest energy MLCT band is clearly red-shifted relative to its position in the osmium monometallic complexes upon coordination of the second metal center and can be attributed to stabilization of the π^* levels of the BL due to interaction with the second $\text{Os}(\text{bpy})_2^{2+}$ moiety.

Slightly higher in energy than the $\text{Os}(\text{d}\pi) \rightarrow \text{BL}(\pi^*)$ MLCT transitions are a series of additional MLCT bands. However, the energy of these bands remains essentially constant as the BL is varied from dpp to dpq to dpb (432, 428, and 422 nm, respectively), indicating that these transitions terminate in a π^* orbital localized principally on the bpy ligand, $\text{Os}(\text{d}\pi) \rightarrow \text{bpy}(\pi^*)$ MLCT. Similar bands are observed in the previously studied $\text{Os}(\text{II})/\text{Ru}(\text{II})$ mixed-metal systems.⁴

Spectroelectrochemistry. With each Os complex it was possible to reversibly oxidize through the first metal-centered oxidation ($\text{Os}(\text{II})/\text{Os}(\text{III})$). Oxidation of $[(\text{bpy})_2\text{Os}]_2(\text{dpp})^{4+}$ to 1100 mV, $[(\text{bpy})_2\text{Os}]_2(\text{dpq})^{4+}$ to 1125 mV, and $[(\text{bpy})_2\text{Os}]_2(\text{dpb})^{4+}$ to 1100 mV resulted in color changes of purple to reddish/purple for the dpp complex, aquamarine to light aquamarine for the dpq complex, and forest green to light green for the dpb complex after passage of approximately 1 equiv of charge each. In all cases oxidation can be reversed by changing the electrolysis potential to 0.0 V with greater than 95% regeneration of the original species. Spectroelectrochemical results are shown in Figures 4-6.

$[(\text{bpy})_2\text{Os}]_2(\text{dpp})^{4+}$ exhibits absorption maxima at 286, 356 (sh), 432, and 552 nm. The lowest energy transition at 552 nm decreases in intensity upon one-electron oxidation. Additionally, the $\text{Os} \rightarrow \text{bpy}$ MLCT at 432 nm is dramatically affected. Oxidation of one metal center to $\text{Os}(\text{III})$ should cause the remaining intensity of the $\text{Os} \rightarrow \text{bpy}$ transition to shift to higher energy, which then appears as a shoulder on the ligand-based $\pi \rightarrow \pi^*$ transitions. Upon two-electron oxidation, loss of the lowest energy transition (552 nm) and the peak at 452 nm is observed, confirming their assignment as $\text{Os}(\text{d}\pi) \rightarrow \text{BL}(\pi^*)$ and $\text{Os}(\text{d}\pi) \rightarrow \text{bpy}(\pi^*)$ charge-transfer transitions.

The intense higher energy bands at 286 and 356 nm for the parent compound do not appear to change in intensity upon one-electron oxidation of the metal center, confirming their assignment as ligand-based transitions. Transitions in this region have previously been assigned as overlapping $\pi \rightarrow \pi^*$ and $n \rightarrow \pi^*$ transitions localized on the bridging and nonbridging ligands.⁴ These bands shift to lower energy in the two-electron-oxidized species as well as decreasing slightly in intensity. Upon oxidation of both metal centers, a new transition appears at about 700 nm which could be due to a ligand-to-metal charge transfer as has been observed in other bimetallic osmium complexes.³⁶ It was not possible to reversibly reduce and reoxidize $[(\text{bpy})_2\text{Os}]_2(\text{dpp})^{4+}$.

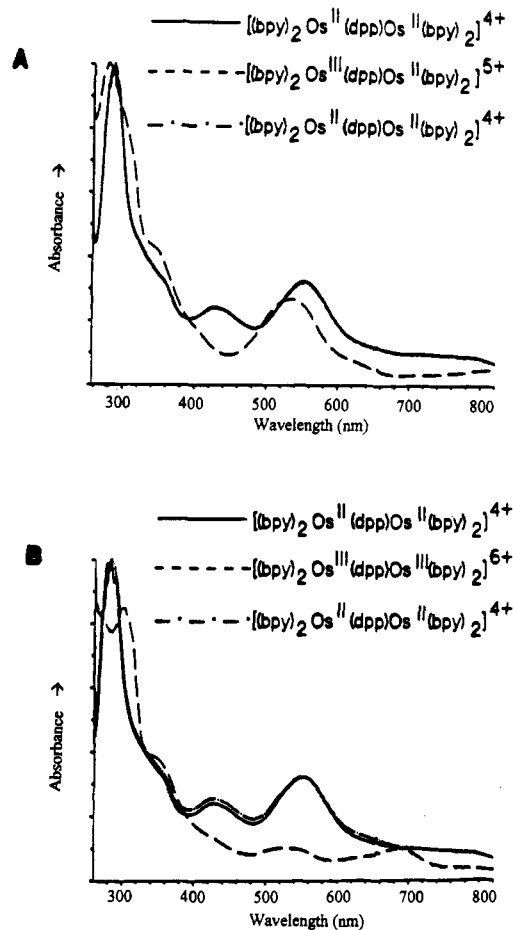


Figure 4. Spectroelectrochemical results for $[(\text{bpy})_2\text{Os}]_2(\text{dpp})(\text{PF}_6)_4$ in CH_3CN (0.1 M Bu_4NPF_6): (A) (—) original spectrum, (---) spectrum after oxidation with approximately 1 equiv of charge to 1.100 V, and (-·-) spectrum after rereduction with 1 equiv of charge to 0.0 V; (B) (—) original spectrum, (---) spectrum after oxidation with approximately 2 equiv of charge to 1.500 V, and (-·-) spectrum after rereduction with 2 equiv of charge at 0.0 V.

In $[(\text{bpy})_2\text{Os}]_2(\text{dpq})^{4+}$ changes in the absorption intensity of the transitions at 630, 428, and 398 nm occur upon one-electron oxidation to form the $\text{Os}(\text{II})/\text{Os}(\text{III})$ species, indicative of $\text{M} \rightarrow \text{bpy}$ and $\text{M} \rightarrow \text{BL}$ MLCT transitions. The transitions at 358 and 286, on the other hand, do not appear to diminish in intensity, hence their assignment as ligand-based transitions.³⁶ The transition at 428 nm experiences a decrease in intensity and a shift to higher energy upon oxidation of only one metal center and is lost upon oxidation of both metal centers, consistent with its $\text{Os} \rightarrow \text{bpy}$ MLCT assignment. Partial loss of absorption intensity between 390 and 450 nm indicates that transitions in this region are both ligand and metal centered or that transitions have been shifted into this region upon electrochemical oxidation of the metal centers. As in the dpp complex, red shifts are observed in the high-energy transition at 286 nm and the lower

(34) (a) Ferguson, J.; Herren, F.; Krausz, E. R.; Vrbancich, J. *Coord. Chem. Rev.* **1985**, *64*, 21. (b) Bryant, G. M.; Ferguson, J. E. *Aust. J. Chem.* **1971**, *24*, 275.
(35) (a) Pankuch, B. J.; Lacky, D. E.; Crosby, G. A. *J. Phys. Chem.* **1980**, *84*, 2061. (b) Lacky, D. E.; Pankuch, B. J.; Crosby, G. A. *J. Phys. Chem.* **1980**, *84*, 2068.

(36) Haga, M.; Matsumura-Inoue, T.; Yamabe, S. *Inorg. Chem.* **1987**, *26*, 4148.
(37) (a) Rillema, D. P.; Taghdiri, D. G.; Jones, D. S.; Keller, C. D.; Worl, L. A.; Meyer, T. J.; Levy, H. A. *Inorg. Chem.* **1987**, *26*, 578. (b) Constable, E. C.; Raithby, P. R.; Smit, D. N. *Polyhedron* **1989**, *8*, 367. (c) Richter, M. M.; Scott, B.; Brewer, K. J.; Willett, R. W. *Acta Crystallogr., Sect. C* **1991**, *C47*, 2443.
(38) Goldsby, K. A.; Meyer, T. J. *Inorg. Chem.* **1984**, *23*, 3002.
(39) See for example: (a) Joss, S.; Reust, H.; Ludi, A. *J. Am. Chem. Soc.* **1981**, *103*, 981. (b) Magnuson, R. H.; Taube, H. *J. Am. Chem. Soc.* **1972**, *94*, 7213. (c) Richardson, D. E.; Sen, J. P.; Buhr, J. D.; Taube, H. *Inorg. Chem.* **1982**, *21*, 3136. (d) Joss, S.; Burgi, H. B.; Ludi, A. *Inorg. Chem.* **1985**, *24*, 949. (e) Dubicki, L.; Ferguson, J.; Krausz, E. R.; Lang, P. A.; Maeder, M.; Magnuson, R. H.; Taube, H. *J. Am. Chem. Soc.* **1985**, *107*, 2167. (f) Kober, E. M.; Goldsby, K. A.; Narayana, D. N. S.; Meyer, T. J. *J. Am. Chem. Soc.* **1983**, *105*, 4303.

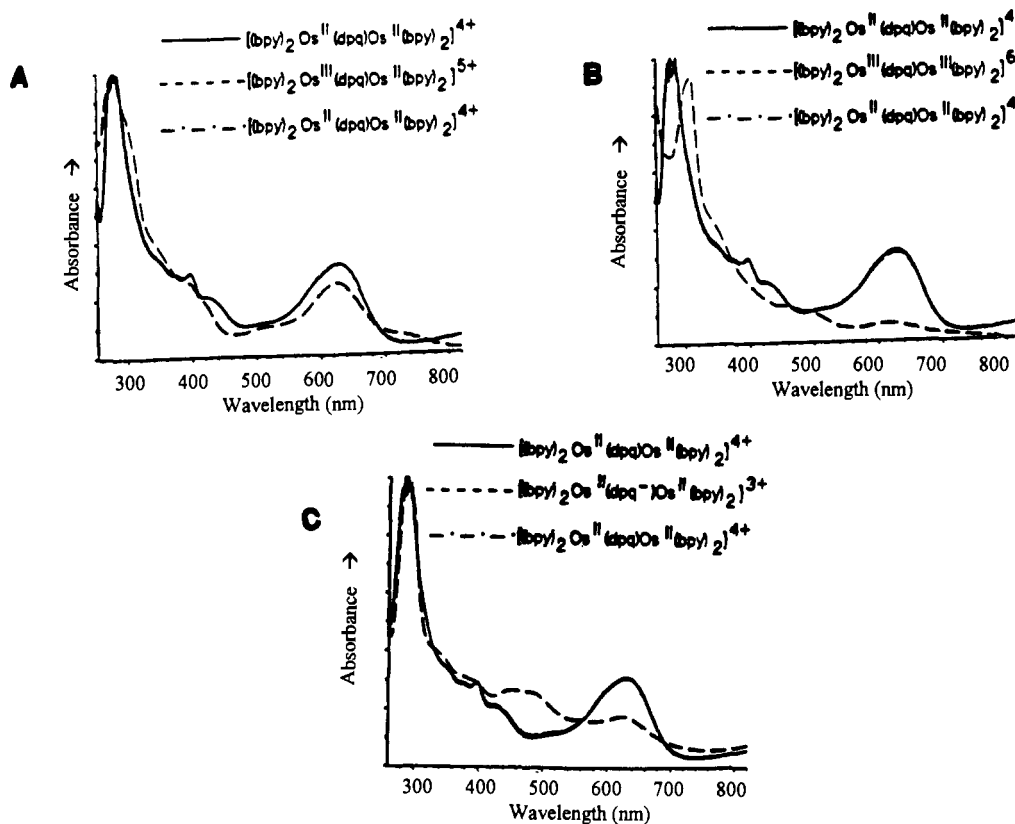


Figure 5. Spectroelectrochemical results for $[(bpy)_2Os]_2(dpq)(PF_6)_4$ in CH_3CN (0.1 M Bu_4NPF_6): (A) (—) original spectrum, (---) spectrum after oxidation with approximately 1 equiv of charge to 1.125 V, and (- · -) spectrum after rereduction with 1 equiv of charge to 0.0 V; (B) (—) original spectrum, (---) spectrum after oxidation with approximately 2 equiv of charge at 1.500 V, and (- · -) spectrum after rereduction with 2 equiv of charge at 0.0 V; (C) (—) original spectrum, (---) spectrum after reduction with approximately 2 equiv of charge at -0.600 V, and (- · -) spectrum after reoxidation with 2 equiv of charge at 0.0 V.

energy shoulder at about 358 nm when the metals are oxidized, which are indicative of bpy- and BL-based $\pi \rightarrow \pi^*$ and $n \rightarrow \pi^*$ transitions.

In $[(bpy)_2Os]_2(dpb)^{4+}$ partial loss of the low-energy transitions at 610 and 670 nm is observed upon one-electron oxidation and is indicative of MLCT transitions. The higher energy transitions at 286 and 354 nm shift to lower energy, indicative of their bpy- and BL-based $\pi \rightarrow \pi^*$ nature, respectively. Upon two-electron oxidation, loss of the lowest energy transitions at 422, 610, and 670 nm is observed, confirming their assignments as $Os \rightarrow bpy$, $Os \rightarrow BL$, and $Os \rightarrow BL$ MLCT in nature, respectively. The higher energy transitions at 354 and 286 nm do not disappear but shift to lower energies, consistent with bpy- and BL-based $\pi \rightarrow \pi^*$ transitions.

One-electron reduction of $[(bpy)_2Os]_2(dpq)^{4+}$ and $[(bpy)_2Os]_2(dpb)^{4+}$ to -600 and -550 mV, respectively, resulted in significant loss of the lowest energy band at 630 and 670 nm in the dpq and dpb complexes, respectively. This confirms their assignment as MLCT transitions in which the π^* -acceptor orbital is BL based. In both the dpq and dpb complexes there is an increase in absorption intensity between the 350- and 550-nm region of the spectrum. This results from a red shift of the $Os \rightarrow bpy$ MLCT upon reduction of the BL. When the BL is reduced, the osmium metal center can no longer efficiently back-bond to the newly occupied π^* orbital on the BL. This results in a more electron-rich metal center, giving rise to the observed red shift of the bpy-based MLCT. A decrease in intensity is observed for the transition at 354 nm in the dpb complex, confirming its assignment as a dpb-based $\pi \rightarrow \pi^*$ transition. The transitions at 286 nm in both the dpq and dpb complexes are not affected by reduction of the BL, giving further support to their assignment as being bpy based.

Correlation of Spectroscopic and Electrochemical Results. A plot of the energies for the lowest energy MLCT transitions (E_{abs} (eV)) versus the difference in redox potentials between the first

Table III. Properties of the Intervalence-Charge-Transfer Bands for $[(bpy)_2Os^{III}(BL)M^{II}(bpy)_2]^{5+}$ (BL = dpq, dpb; M = Os, Ru)^a

M	BL	d (Å)	E_{op} (cm ⁻¹)	ϵ_{max} (M ⁻¹ cm ⁻¹)	$\Delta\nu_{1/2}$ (cm ⁻¹)		α^2
					obsd	calcd	
Os	dpp	7.011	8370	2860	1260	4400	3.7×10^{-3}
		7.011	11,800	4060	3130	5220	1.0×10^{-2}
Os	dpq	7.011	9620	4080	2490	4710	9.0×10^{-3}
Os	dpb	7.011	9260	3840	2440	4620	8.6×10^{-3}
Ru	dpp	7.004	9090	1720	2710	4060	4.4×10^{-3}
Ru	dpq	7.004	8680	1190	2700	4000	3.2×10^{-3}
Ru	dpb	7.004	8200	930	2730	3880	2.7×10^{-3}

^a Spectra were recorded in CH_3CN at room temperature.

metal-based oxidation and first bridging-ligand-based reduction, $\Delta E_{1/2}$ ($E_{1/2}(Os(II)/Os(III)) - E_{1/2}(BL/BL^-)$), for the Os(II) monometallic complexes, $[Os(bpy)_2(BL)]^{2+}$,^{4b} the Os/Ru bimetallic complexes, $[(bpy)_2Os(BL)Ru(bpy)_2]^{4+}$,^{4a} and the Os/Os bimetallic complexes, $[(bpy)_2Os]_2(BL)^{4+}$, gave a linear correlation in which a linear-least-squares analysis yielded

$$E_{abs} = 0.387 \text{ } 10 + 1.1130 \Delta E_{1/2} \quad r = 0.975$$

where r is the correlation coefficient. The linear nature of the plot with a slope near unity indicates that the same $d\pi - \pi^*$ MLCT orbitals are involved in both the optical and electrochemical processes.^{4,40-42}

Near-Infrared Spectra. The one-electron-oxidized homo- and heterobimetallic complexes, $[(bpy)_2Os^{III}(BL)M^{II}(bpy)_2]^{5+}$ (BL = dpq, dpb; M = Os, Ru) exhibit rich near-infrared spectra that are summarized in Table III. It was not possible to reversibly

- (40) (a) Kober, E. M.; Sullivan, B. P.; Dressick, W. M.; Caspar, J. V.; Meyer, T. J. *J. Am. Chem. Soc.* **1980**, *102*, 7385. (b) Caspar, J. V.; Kober, E. M.; Sullivan, B. P.; Meyer, T. J. *J. Am. Chem. Soc.* **1982**, *104*, 630.
 (41) Dodsworth, E. S.; Lever, A. *Chem. Phys. Lett.* **1985**, *119*, 61.
 (42) Saji, T.; Aoyagui, J. *J. Electroanal. Chem. Interfacial Electrochem.* **1975**, *60*, 1.

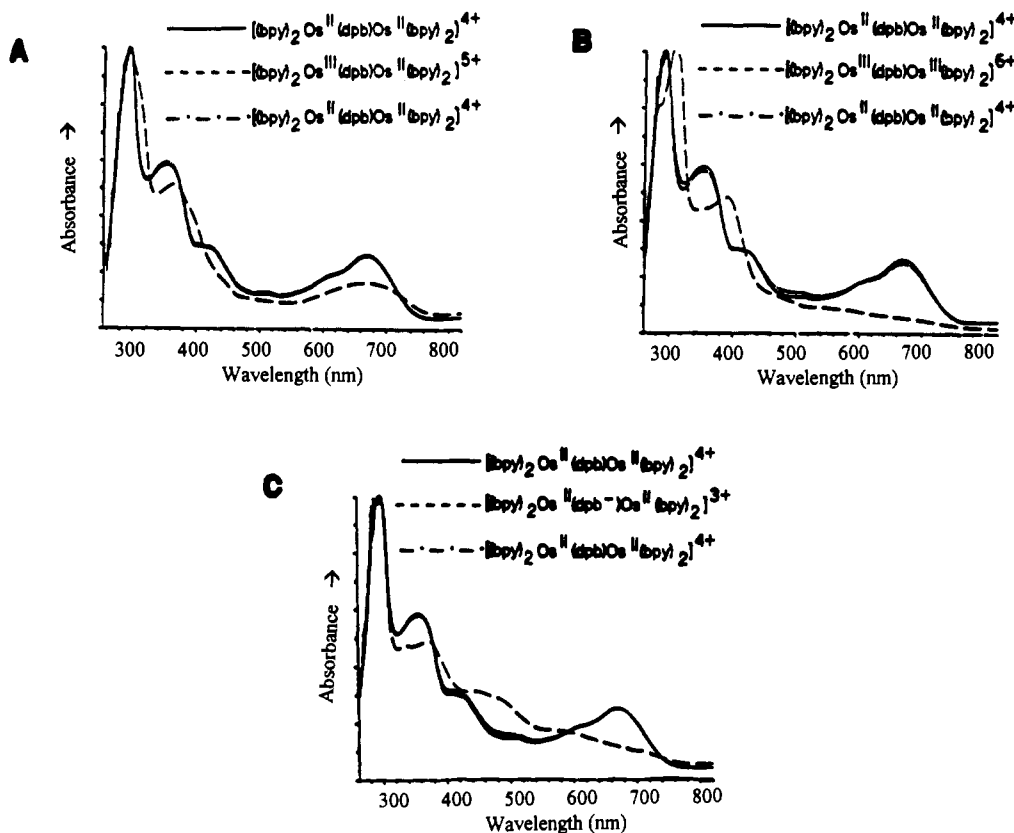


Figure 6. Spectroelectrochemical results for $[(\text{bpy})_2\text{Os}^{\text{II}}(\text{dpb})\text{Os}^{\text{II}}(\text{bpy})_2]^{4+}$ in CH_3CN (0.1 M Bu_4NPF_6): (A) (—) original spectrum, (---) spectrum after oxidation with approximately 1 equiv of charge to 1.100 V, and (-·-) spectrum after re-reduction with 1 equiv of charge to 0.0 V; (B) (—) original spectrum, (---) spectrum after oxidation with approximately 2 equiv of charge at 1.500 V, and (-·-) spectrum after re-reduction with 2 equiv of charge at 0.0 V; (C) (—) original spectrum, (---) spectrum after reduction with approximately 2 equiv of charge at -0.550 V, and (-·-) spectrum after re-oxidation with 2 equiv of charge at 0.0 V.

generate the one electron-oxidized form of the Ru/Ru systems on the longer time scale needed for near-IR analysis. This could result from the more positive potential needed to oxidize the ruthenium metal centers.

The near-IR spectrum of $[(\text{bpy})_2\text{Os}^{\text{III}}(\text{dpp})\text{M}^{\text{II}}(\text{bpy})_2]^{5+}$ reveals the presence of two IT (intervalence-transfer) bands in this spectral region. These multiple IT bands have been observed in the past for complexes containing osmium metal centers.^{36,38,39,43} The semiquantitative analysis of multiple IT bands in $[(\text{bpy})_2\text{ClOs}(\text{PPh}_2\text{CH}_2\text{PPh}_2)\text{OsCl}(\text{bpy})_2]^{3+}$ has shown that the magnitude of the separation between the spin-orbit states is reflected in the separation of the multiple IT bands.

$$E_{\text{SO},1} = E_{\text{IT},2} - E_{\text{IT},1}$$

$$E_{\text{SO},2} = E_{\text{IT},3} - E_{\text{IT},2}$$

On the basis of the spectra obtained for our dpp-bridged osmium system, $E_{\text{SO},1} = 3430 \text{ cm}^{-1}$. The third IT band which yields the $3E'$ spin-orbit state should occur at ca. 3430 cm^{-1} higher energy than IT,2 and would be obscured by the more intense MLCT band in this region. However, a shoulder does appear in this region at ca. 650 nm in the spectroelectrochemistry of this mixed-valence species shown in Figure 4A.

Since the value of E_{SO} is not expected to vary dramatically as the bridging ligand is changed in this series, the other expected IT bands for the dpq- and dpb-bridged systems will lie out of the detection window of the near-IR analysis and only $E_{\text{IT},2}$ is observed, the intervalence transfer leading to the generation of an excited $2E'$ spin-orbit state.

For weakly coupled mixed-valence systems, Hush derived equations describing the expected properties of intervalence bands.⁴⁴ A lower limit for the band width at room temperature

is given by

$$\Delta\nu_{1/2}(\text{calcd}) = [2.31 \times 10^3(E_{\text{op}} - \Delta E)]^{1/2}$$

where $\Delta\nu_{1/2}(\text{calcd})$ is the lower limit for the full width at half-maximum, ΔE is the internal energy difference between sites, and E_{op} is the energy of the IT band.⁴⁴ Calculated half-widths are given in Table III. All of the $\Delta\nu_{1/2}$ observed are significantly less than those calculated and probably result from the large degree of overlap of the IT bands on the tails of MLCT transitions.

In an elegant study by Meyer and Goldsby, a relationship between intervalence absorption energies and redox asymmetry of a series of Ru/Ru and Os/Ru complexes was observed.³⁸

$$\Delta E_{\text{op}} = \Delta(\Delta E_{1/2})$$

$$\Delta E_{\text{op}} = E_{\text{op}}(\text{Ru}^{\text{II}}/\text{Os}^{\text{III}}) - E_{\text{op}}(\text{Ru}^{\text{II}}/\text{Ru}^{\text{III}})$$

$$\Delta(\Delta E_{1/2}) = \Delta E_{1/2}(\text{Ru}/\text{Os}) - \Delta E_{1/2}(\text{Ru}/\text{Ru})$$

These systems all involve IT transitions that generated a new d^5 ion on a ruthenium center which has a much lower SO state than osmium. Hence, all of the systems studied exhibited a single IT band, although this band represents overlapping SO components. In the absence of observation of all of the SO components in the Os/Os systems, quantitative analysis of this relationship is not possible. It is, however, possible to see that the energy of the first component of the series of IT bands in the dpp-bridged Os complex, $E_{\text{IT},1}$, is less than E_{op} for the analogous Os/Ru system. This is consistent with the higher value of the redox asymmetry of this mixed-metal system.

(43) Kober, E. M.; Goldsby, K. A.; Narayana, D. N. S.; Meyer, T. J. *J. Am. Chem. Soc.* **1983**, *105*, 4303.

(44) (a) Hush, N. S. *Trans. Faraday Soc.* **1961**, *57*, 557. (b) Hush, N. S. *Prog. Inorg. Chem.* **1967**, *8*, 391. (c) Hush, N. S. *Electrochim. Acta* **1968**, *13*, 1005.

The extent of electron delocalization, α^2 , can be estimated from these spectra using the equation derived by Hush⁴⁴

$$\alpha^2 = \frac{(4.2 \times 10^{-4}) \epsilon_{\max} \Delta\nu_{1/2}}{d^2 E_{\text{op}}}$$

where $\Delta\nu_{1/2}$ is the bandwidth at half-intensity, ϵ_{\max} is the extinction coefficient ($\text{M}^{-1} \text{cm}^{-1}$), d is the intermetallic distance (\AA), and E_{op} is the energy of the intervalence (IT) transition (cm^{-1}). The values for the parameters for both the homometallic Os(II)/Os(III) and heterometallic Os(III)/Ru(II) complexes are located in Table III. The value for d was estimated at 7.011 \AA for the Os/Os systems by accounting for the 0.007- \AA difference of the Os–N and Ru–N distances from the X-ray crystal structure data for $[\text{M}(\text{bpy})_3]^{2+}$ and utilizing the Ru–N and N–N (pyrazine) distances from the X-ray crystal structure data for the monometallic $[\text{Ru}(\text{bpy})_2(\text{dpq})]^{2+}$ complex.³⁷ The value of d obtained for the Os/Ru complexes was obtained by using the value for the Os–N distances mentioned above and obtaining the Ru–N and N–N (pyrazine) distances from the crystal structure of $[\text{Ru}(\text{bpy})_2(\text{dpq})]^{2+}$. The small values obtained for α^2 are similar to those observed for other osmium and ruthenium polypyridyl-bridged systems,^{29,36,38} and indicate that electronic coupling is weak between sites. The very low values of α^2 compared to the larger values of K_{com} are also observed for Os/Ru and Ru/Ru systems bridged by pyrazine and bipyrimidine.³⁸ These values indicate that K_{com} is dominated by electrostatics and solvation energy in the electrochemical experiment and electronic coupling between the sites is weak.

For the three Os(II)/Os(III) systems, little change is observed in the degree of delocalization, which is in good agreement with the electrochemical data presented above. It is interesting to note that the general trend is a decreased extent of delocalization as the bridging ligand is varied from dpp to dpq to dpb. This observed decrease in coupling as the energy of the bridging ligand LUMO is stabilized (i.e. brought closer in energy to the Os($d\pi$) orbital) is somewhat surprising. The nature of the bridging ligand LUMO varies from dpp to dpq as illustrated by Wertz et al.² Wertz indicates that the LUMO on dpp is based on both the pyrazine and pyridine moieties of the ligand while the dpq LUMO localizes on the quinoxaline portion of the ligand. By analogy, the LUMO on dpb is expected to localize primarily on the benzoquinoxaline portion of the ligand. Hence, the LUMO of these bridging ligands localizes away from the nitrogens coordinated to the metal centers through the series dpp to dpq to dpb. This appears to counteract the lowering of the energy of the bridging-ligand-based π^* orbital and gives rise to the decreased α^2 values from dpp to dpq to dpb.

Comparison of the three heterometallic Os/Ru systems to the three homometallic Os/Os systems shows a higher degree of delocalization in the all osmium systems. This is consistent with the available electrochemical measurements of the homometallic Os/Os and Ru/Ru systems which indicate a larger degree of

communication in the osmium systems. This smaller value of α^2 for the mixed-metal systems indicates that the Ru metal center dominates the coupling between the sites and that its lower energy $d\pi$ orbital gives rise to a decreased coupling through the bridging ligand in a "superexchange" mechanism than the analogous higher energy Os $d\pi$ orbital. This spectroscopic evidence for the mixed-metal systems is the first available measure of the degree of coupling in these mixed-metal systems and indicates that the all osmium systems have a much larger degree of coupling than the mixed-metal Os/Ru systems.

Conclusions

Comparison of the electrochemical and spectroscopic data for these bimetallic complexes shows that addition of a second metal center to the $[\text{Os}(\text{bpy})_2(\text{BL})]^{2+}$ parent compound results in a shift of the MLCT absorption maxima to lower energies with a subsequent decrease in the reduction potential for the first bridging-ligand-based reductions. In general, the metal-centered properties are relatively unaffected by the presence of a metal fragment on the other side of the bridging ligand as compared with those properties sensitive to the energy of the BL-based π^* orbital, which have been shown to be greatly affected by the number and type of metals bound to the system. The intervalence-charge-transfer studies indicate that the metal–metal coupling is enhanced in these all-osmium systems relative to the osmium/ruthenium mixed-metal analogs, consistent with a through-bridge "superexchange" mechanism in which the higher energy Os $d\pi$ orbitals facilitate mixing. This indicates that substitution of the metal center in complexes of this type will affect the degree of metal–metal coupling provided by the bridging ligand. Most notably, the intervalence studies indicate that the large K_{com} values obtained from the electrochemical studies are dominated by electrostatic and solvation effects and these bridging ligands appear to provide rather limited delocalization in the mixed-valence forms. The stability of several oxidation states in these complexes has made it possible to perform spectroelectrochemical experiments which have clarified both the electronic spectra and electrochemical data. In addition, this property makes these systems of interest for utilization in catalysis of multielectron processes. On the basis of spectroelectrochemical, near-infrared, and electrochemical experiments these complexes have been shown to be Robin and Day Class II systems. Continuing study of these compounds and their higher order polymetallic derivatives will be the subject of a forthcoming report.⁴⁵

Acknowledgment. We thank Dr. Scot Wherland for his help in obtaining the intermetallic distance used in the calculations of α^2 and Johnson Matthey for the loan of the ruthenium trichloride used in this study. This work was supported in part by funds provided by Virginia Polytechnic Institute and State University, Washington State University, and the National Science Foundation (Grant CHE-9108374).

(45) Richter, M. M.; Brewer, K. J. Manuscript in preparation.